Available online at www.sciencedirect.com
SCIENCE DIRECT®

Journal of the European Ceramic Society 24 (2004) 1181–1185

www.elsevier.com/locate/jeurceramsoc

Delay of tetragonal-to-monoclinic transition in water vapour due to nanostructural effect

F. Boulc'h*, L. Dessemond, E. Djurado

Laboratoire d'Electrochimie et de Physico-chimie des Matériaux et des Interfaces 1130, rue de la Piscine- BP 75, 38402 Saint-Martin d'Héres Cedex, France

Abstract

The ageing behaviour of ultrafine yttria-doped single-phased tetragonal zirconia was investigated at 400 °C in dry air and in water vapour by complex impedance analysis and Raman spectroscopy. Pellets sintered at 1500 °C for 2 h in air were characterized by a 60 nm average grain size, a unimodal distribution of 300 nm average aggregate size, a density of 97% of theoretical one and pore sizes lower than 20 nm. No degradation of the electrical properties of dense pellets was detected in both gaseous environments during 1000 h at 400 °C. Simultaneously, no monoclinic signature was detected by Raman spectroscopy. Furthermore, tests were investigated in conditions close to those of IT-SOFC: 700 °C in water vapour during 1000 h. In these conditions, a conductivity decrease of 5% was recorded and less than 2 mol% of monoclinic zirconia was observed by Raman spectroscopy.

Keywords: Electrical properties; Fuel Cell; Grain size; Y_2O_3; ZrO_2

1. Introduction

At present, efforts are focused on lowering the operating temperature of solid oxide fuel cells (SOFC) from above 900 °C down to 700 °C (IT-SOFC). Tetragonal zirconia (TZP) is considered as a promising candidate to be used as electrolyte in IT-SOFC, because of its good mechanical and electrical properties with comparison to cubic zirconia. However, the major drawback of TZP is the low temperature degradation caused by tetragonal to monoclinic phase transition (t-m) accompanied by microcraks which are due to an acceleration of grain growth in water vapour.[1–3] Badwal et al. [4] predicted that the t-m transition was controlled by microstructural parameters such as grain size, grain size distribution and porosity. Up to now, all sintered TZP ceramics undergo the tetragonal-monoclinic phase transition between 100–500 °C.[5]

Considering the accurate analysis of densification of yttria-stabilized zirconia by impedance spectroscopy [6] and its capability to phase detection in zirconia based ceramics,[7] this technique can be regarded as a powerful tool to monitor the tetragonal zirconia destabilization.

The first aim of this work is to investigate the tetragonal zirconia ageing behaviour in dry air and in water vapour at 400 °C during 1000 h. Impedance spectroscopy measurements were completed by Raman spectroscopy, in order to detect both tetragonal and monoclinic symmetries. Secondly, tests were performed in nearly IT-SOFC conditions. Thus, ageing was characterized at 700 °C in water vapour during 1000 h.

2. Experimental

Yttria-doped zirconia powder was prepared by the spray-pyrolysis technique using an ultrasonic atomizer. The precursor solutions were prepared from stoichiometric mixture of zirconyl nitrate hydrate and yttrium nitrate in distilled water. Stoichiometry of powder—$(ZrO_2)_{0.975}(Y_2O_3)_{0.025}$—was found to be similar to the precursor solution, as measured by inductively coupled plasma emission spectroscopy (ICP). Microscopic scanning observations show smooth submicronic spherical particles dense and homogeneous in composition.[8] As prepared powders were cold isostatically pressed at 300 MPa and sintered at 1500 °C for 2 h in air (heating and cooling rate: 10 °C min^{-1}). The final stoichiometry of

* Corresponding author. Tel.: +33-04-76-82-66-84; fax: +33-04-76-82-67-77.
E-mail address: florence.boulch@lepmi.inpg.fr (F. Boulc'h).

0955-2219/$ - see front matter © 2003 Elsevier Ltd. All rights reserved.
doi:10.1016/S0955-2219(03)00563-6

sintered pellets was determined by electron probe microanalysis (CAMECA SX 50, 200 nA, 15 kV) using $(ZrO_2)_{0.92}(Y_2O_3)_{0.08}$ ceramic as the standard. A 2 μm^3 volume was examined with a sensibility of 1000 ppm. Mass percent was determined from ten experimental points. The microstructure of ceramics was examined using scanning electron microscopy (SEM Jeol JSM-35). Nitrogen adsorption/desorption experiments were performed at −196 °C using a static volumetric method (Micrometric ASAP 2010) in order to determine pore size. Nitrogen adsorption/desorption was carried out in the relative pressure range of $10^{-7} < p/p0 < 1$. Before measurements, samples were cleaned in vacuum at 105 °C by helium flushing. Mesopore surface areas were determined from the BJH (Barett–Joyner–Hallenda) method.[9] The micropore surface and volume were calculated from the t-plot method within the relative pressure $0.01 < p/p0 < 0.65$.[10] Density was measured from the size and the weight of the samples. X-Ray diffraction was carried out in order to determining the average grain size and the unit cell parameters, using a Siemens D500 $\theta/2\theta$ diffractometer equipped with a linear detector (CuK_α radiation, $\lambda = 1.54$Å, from 20 to 80°, 0.04°/2θ steps, 6 s counting time). The crystalline domain size is calculated by the Scherrer formula, applied to *111* peak and valid as long as the crystalline domain size is smaller than 100 nm. Position and Full Width at Half Maximum (FWHM) of *111* peak were determined by a deconvolution of pseudo-Voigt-shaped peaks with Profile fitting software (Diffractat, Socabim). Room temperature micro-Raman spectra were recorded on a DILOR XY confocal Raman spectrometer equipped with a charge-coupled device (CCD) array detector, using the 514.5 nm line of an argon ion laser. All experiments were carried out using a laser power of 20 mW. Less than 5 mol% traces of monoclinic form can be detected by Raman spectroscopy. Impedance spectroscopy measurements were performed on symmetrical pellet in dry air first and then in water vapour. Platinum coatings were deposited on both sides of pellet by radio frequency sputtering (Plassys MP300) at room temperature in order to obtain homogeneous and porous coatings without any heating treatment before electrical measurements. Platinum grids were used as current collectors. Impedance diagrams were recorded under zero dc conditions in the 5–1.3×10^7 Hz frequency range using a Hewlett-Packard impedancemeter (HP 4192LF). The amplitude of the measuring voltage was 200 mV. The working temperature in the furnace was controlled within ±1 °C. The impedance diagrams were resolved in individual components by using Zview software (version 2.1, Scribner Associates).

3. Results and discussion

3.1. Material

1. The stoichiometry of sintered ceramics was similar to that of powders (Table 1). Pellets were characterized by a high purity. No trace of silica was detected and batches contained only traces of hafnium. The good homogeneity in composition of the pellet was evidenced by weak values of the standard deviation (<0.5%).
2. A unimodal distribution of 300 nm average spherical particles size was determined by SEM observations (Fig. 1a). As shown by previous HRTEM observations,[11] these latter are aggregates of single crystals conventionally called grains.
3. Density was found to be equal to 97% of the theoretical one and the pore size is always lower

Table 1
Physico-chemical characterizations of TZP ceramics

Stoichiometry	Electron probe microanalysis		*Mass% theoretical*	*Mass% measured*
		Y	3.6	3.6±0.1
		Zr	70.6	69.7±0.3
		O	25.8	26.1±0.4
Density	Size: $d = 6.1$ mm/$e = 2.1$ mm Weight: 0.355 g	*ρ theoretical*	*ρ experimental*	*Density*
		5.94 g.cm^{-3}	5.74 g.cm^{-3}	97%
Porosity	Nitrogen adsorption/desorption Pellet volume:61 mm^3		*Pore size*	*Total volume*
		Micropore	<2 nm	0.1 mm^3
		Mesopore	20 nm	2 mm^3
	Scherrer formula $L = 0.9^*\lambda/(\Delta\theta^*\cos\theta_0)$ $\Delta\theta = \left(\mathrm{FWHM}^2_{\mathrm{sample}} - \mathrm{FWHM}^2_{\mathrm{Si}}\right)^{1/2}$	*2 θ₀*	$FWHM_{sample}$	$FWHM_{Si}$
		30.30°	1.3204°	0.1615°
		Average grain size: 62.8 nm±1.6 nm		

than 20 nm (Table 1), as observed by microscopy observation (Fig. 1b).

4. After sintering at 1500 °C for 2 h, a 60 nm average grain size was determined (Table 1). The unit-cell parameters are equal to a = 0.508 nm and c = 0.516 nm respectively. The c/a value of 1.015 confirms the tetragonality of the investigated sample.
5. Within the experimental accuracy, Raman spectrum reveals tetragonal single-phased zirconia, free of monoclinic phase (Fig. 2a).

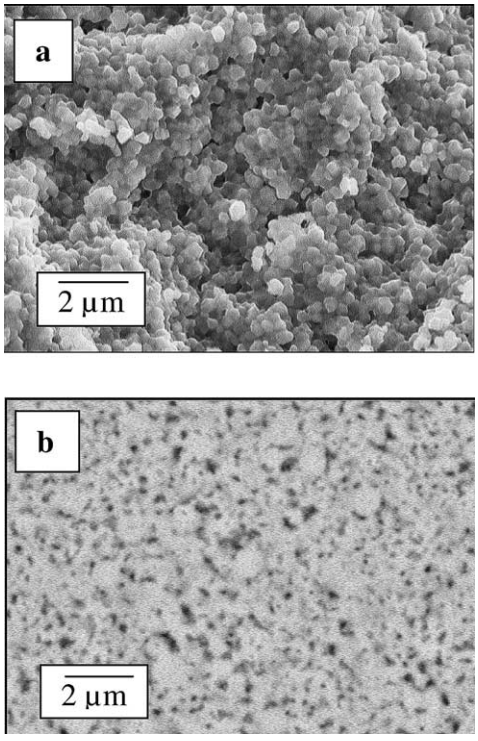

Fig. 1. Morphology of $(ZrO_2)_{0.975}(Y_2O_3)_{0.025}$ (a) ceramic (b) polished ceramic observed by SEM.

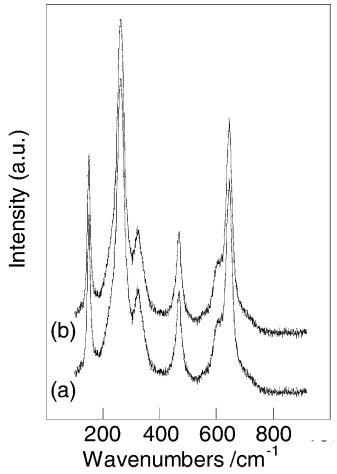

Fig. 2. Raman spectrum of $(ZrO_2)_{0.975}(Y_2O_3)_{0.025}$ (a) before ageing treatment (b) after 1000 h at 400 °C in water vapour.

4. Impedance spectroscopy

A typical impedance diagram recorded on tetragonal single-phased yttria-doped zirconia is composed of two-well separated semi-circles (Fig. 3). The high frequency semicircle is related to the specific electrical properties of zirconia grains and the low frequency one describes the blocking effect due to regular grain boundaries. The depression angle for the bulk semicircle is lower than 10° indicating a good homogeneity of the electrical properties of the grains and thus of their composition. The blocking process depression angle is also quite low, demonstrating a high homogeneity of the blocking characteristics and therefore a narrow pore size distribution, in agreement with microscopic observations.

4.1. Ageing in dry air at 400 °C for 1000 h

The scattering on measured impedances, and related electrical components of both electrolyte contributions, was evaluated to 2% by plotting successive impedance diagrams during the early stage of the ageing period in dry air, characterized by low water content (< 10 ppm). It is likely to be due to fluctuations in the working temperature around 400 °C, as further confirmed by electrical measurements during isothermal ageing. After 1000 h, only a weak increase of 1% of the blocking resistance was observed whereas the specific resistance remains unchanged. However, this variation is lower than experimental scattering and cannot thus be regarded as significant. The specific and blocking capacitances (and therefore the corresponding relaxation frequencies) are identically constant within the whole ageing period. Moreover, no significant variation of the depression angle of both electrolyte contributions was recorded. Nevertheless, in the literature, an increase of the depression angle was recorded in stabilized zirconia. This behaviour was explained as the appearance of cracks resulting from its ageing.[12]

4.2. Ageing in water vapour at 400 °C for 1000 h

For the water vapour ageing, dry air flew in water bath and spread in furnace with a flow rate of 10 ml h^{-1}. As

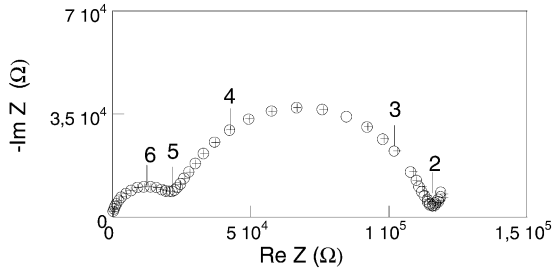

Fig. 3. Electrolyte impedance of $(ZrO_2)_{0.975}(Y_2O_3)_{0.025}$ at 400 °C in water vapour: ○ Before ageing / + after 1000 h.

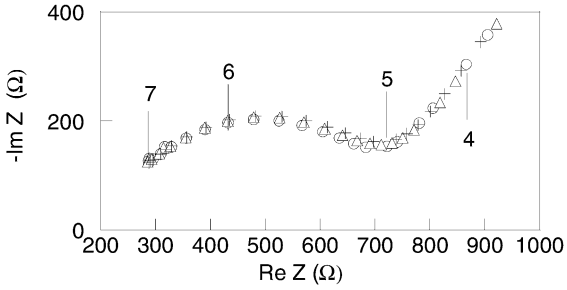

Fig. 4. Electrolyte impedance of $(ZrO_2)_{0.975}(Y_2O_3)_{0.025}$ at 700 °C in water vapour: ● Before ageing/Δ after 600 h /+after 1000 h.

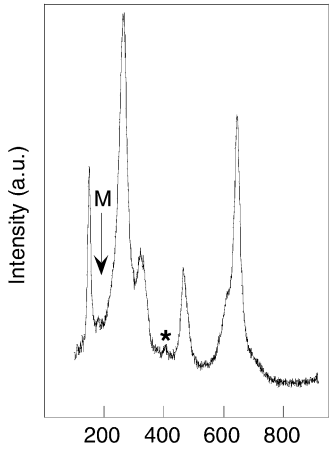

Fig. 5. Raman spectrum of $(ZrO_2)_{0.975}(Y_2O_3)_{0.025}$ after an ageing of 1000 h at 700 °C in water vapour. * : Fluorescence.

water bath temperature is maintained to 20 °C, gaseous environment is characterized by 2% of water vapour.

Surprisingly enough, no variation of all electrical parameters was recorded during ageing for 1000 h at 400 °C (Fig. 3). These results unambiguously prove that neither microstructural modification (in terms of grain size and porosity) nor structural variation (in terms of second phase) occurred in the chosen experimental conditions. This was confirmed by Raman spectroscopy, which reveals only tetragonal single-phased zirconia, without any monoclinic traces after both ageing treatments in dry air and water vapour atmospheres (Fig. 2b). In contradiction with literature data, it is worth emphasizing that the investigated samples do not destabilize. Inhibition of tetragonal-to-monoclinic transformation is likely to be controlled by nanometric grain size, nanoporosity, high density and good homogeneity both in composition and size.

4.3. Ageing in IT-SOFC conditions: at 700 °C in water vapour for 1000 h

After 1000 h, only a slight decrease of 5% of the yttria-doped zirconia conductivity was recorded, as shown in Fig. 4. Moreover, less than 2 mol% of monoclinic zirconia was detected by Raman spectroscopy (Fig. 5). These results further confirm the potential application of nanocrystalline yttria doped TZP as electrolyte for IT-SOFC.

5. Conclusion

Whatever the ageing environment, the electrical properties of nanometric single phased tetragonal zirconia were not altered for times up to 1000 h at 400 °C. No significant modification of the microstructural parameters was detected. Moreover, Raman spectroscopy confirmed that the tetragonality of investigated samples remained unchanged. The inhibition of the tetragonal to monoclinic transition seems to be controlled by nano-scaled material (grain size and porosity). At 700 °C, in water vapour, after 1000 h, only a weak decrease of conductivity is observed due to the appearance of less than 2 mol% of monoclinic zirconia. Moreover, coupling impedance and Raman spectroscopies can be implemented to detect the tetragonal phase destabilization in zirconia based ceramics.

Acknowledgements

We gratefully thank Dr K. Wodnicka and Pr K. Haberko from the University of Materials Science and Ceramics in Cracow for their contribution to nitrogen adsorption / desorption measurements.

References

1. Lange, F. F., Dunlop, G. L. and Davis, B. I., Degradation during aging of transformation-toughened ZrO_2-Y_2O_3 Materials at 250 °C. *J. Am. Ceram. Soc.*, 1986, **69**, 237–240.
2. Murase, Y. and Kato, E., Role of water vapor in crystalline growth and tetragonal-monoclinic phase transformation of ZrO_2. *J. Am. Ceram. Soc.*, 1983, **66**, 196–200.
3. Sato, T. and Shimada, M., Transformation of yttria-doped tetragonal ZrO_2 polycrystals by annealing in water. *J. Am. Ceram. Soc.*, 1985, **6**, 356–359.
4. Badwal, S. P. S. and Nardella, N., Formation of monoclinic zirconia at the anodic face of tetragonal zirconia polycrystalline solid electrolyte. *Appl. Phys. A*, 1989, **49**, 13–24.
5. Lawson, S., Environmental degradation of zirconia ceramics. *J. Eur. Ceram. Soc.*, 1995, **15**, 485–502.
6. Steil, M. C., Thévenot, F. and Kleitz, M., Densification of yttria-stabilized zirconia impedance spectroscopy analysis. *J. Electrochem. Soc.*, 1997, **144**, 390–396.
7. Mucillo, E. N. S. and Kleitz, M., Impedance spectroscopy of Mg-partially stabilized zirconia and cubic phase decomposition. *J. Eur. Ceram. Soc.*, 1996, **16**, 453–465.
8. Boulc'h, F. and Djurado, E., Structural changes of rare-earth doped nanostructured zirconia solid solution. *Solid State Ionics*, 2002 in press.

9. Barett, E. P., Joyner, L. G. and Halenda, P. P., *J. Am. Chem. Soc*., 1951, **73**, 373.
10. Lippens, B. C. and de Boer, J. H., *J. Cat*., 1965, **4**, 319–323.
11. Boulc'h, F., Schouler, M. C., Donnadieu, P., Chaix, J. M. and Djurado, E., Domain size distribution of Y-TZP nano-particles using XRD and HRTEM. *Image Anal Stereo*, 2001, **20**, 157–161.
12. Dessemond, L. and Kleitz, M., Effect of mechanical damage on the electrical properties of zirconia ceramics. *J. Eur. Ceram. Soc*., 1992, **9**, 35–39.